COMMUN. MATH. SCI.
Vol. 20, No. 8, pp. 2207–2230

ON BV-INSTABILITY AND EXISTENCE FOR LINEARIZED RADIAL EULER FLOWS*

HELGE KRISTIAN JENSSEN† AND YUSHUANG LUO‡

Abstract. We provide concrete examples of immediate BV-blowup from small and radially symmetric initial data for the 3-dimensional, linearized Euler system. More precisely, we exhibit data arbitrarily close to a constant state, measured in L-infinity and BV (functions of bounded variation), whose solution has unbounded BV-norm at any positive time. Furthermore, this type of BV-instability can occur in the absence of any focusing waves in the solution. We also show that the BV-norm of a solution may well remain bounded while suffering L-infinity blowup due to wave focusing. Finally, we demonstrate how an argument based on scaling of the dependent variables, together with 1-d variation estimates, yields global existence for a class of finite energy, but possibly unbounded, radial solutions.

Keywords. Multi-dimensional systems of hyperbolic PDEs; radial solutions; BV-instability.

AMS subject classifications. 35L45; 35B44.

1. Introduction

In the first part of this work we consider the issue of BV-instability for the 3-dimensional, linearized compressible Euler system. As a constant coefficients, first-order symmetrizable system with non-commuting Jacobians, it follows from a theorem of Brenner [1] that the Cauchy problem is unstable in L^p whenever $p \neq 2$. The results in [1] generalized earlier results of Littman [17, 18] specifically for the wave equation in more than one space dimension. This result was later used by Rauch [19] to establish that BV-stability (in the sense of (1.1) below) requires commutativity also for *non-linear*, symmetrizable systems in more than one space dimension.

Brenner's and Rauch's abstract arguments apply to general systems. In this work, our first goal is to provide concrete examples of (violent) BV-instability for the particular case of the linearized Euler system in $\mathbb{R}^3$. Motivated by De Lellis' more recent work [6] on BV-blowup for so-called Keyfitz-Kranzer systems, we show that *immediate* BV-blowup can be achieved from initial data that are arbitrarily small in both $BV(\mathbb{R}^3)$ and $L^\infty(\mathbb{R}^3)$.

It is well known that the compressible Euler system admits solutions that undergo wave-focusing. In particular, *radial* solutions may suffer blowup in L^∞ (see [14] for the classic case of radial similarity solutions first considered by Guderley [9]). It has been indicated in the literature (e.g., introductions in [12, 13]) that the phenomenon of focusing is incompatible with BV-stability. Our examples illustrate, at the linearized level, that the situation is somewhat more subtle.

We first exhibit a case in which the BV-norm of a focusing solution remains bounded, while suffering blow up in L^∞ (see Section 3.1). The possibility of this behavior relies on the fact that, in dimension $d>1$, $BV_{loc}(\mathbb{R}^d)$ contains unbounded functions. For example, a standard calculation shows that, for the unit ball B_1 in $\mathbb{R}^d$, the radial function $|\mathbf{x}|^{-\mu}$ is an unbounded element of $W^{1,1}(B_1) \subset BV(B_1)$ whenever $0<\mu<d-1$ (see Ex. 5.2.3 in [7] and Section 13.1 in [16]).

*Received: October 10, 2021; Accepted (in revised form): March 01, 2022. Communicated by Mikhail Feldman.

†Department of Mathematics, Penn State University, University Park, State College, PA 16802, USA (jenssen@math.psu.edu).

‡Department of Mathematics, Penn State University, University Park, State College, PA 16802, USA (yzl55@psu.edu).

We then give an example which shows how initial data that are arbitrarily close to a constant in both amplitude and variation can generate immediate BV-blowup, even in the absence of any focusing waves (see Section 3.2). Thus, contrary to what may appear to be a reasonable guess, BV instability is not directly related to wave focusing.

REMARK 1.1 (Relevance of BV-instability). Glimm's celebrated theorem [8] on global existence of weak solutions for 1-d conservative systems applies to strictly hyperbolic systems and provides an estimate of the form

$$\operatorname{Var} u(t) \leq Const. \operatorname{Var} u_0, \tag{1.1}$$

whenever $\operatorname{Var} u_0$ is sufficiently small. The results of Brenner [1] and Rauch [19] show that the same type of bound is not available in multi-d, unless the Jacobians of the fluxes in different spatial directions commute ("commuting systems"). As it turns out, a BV-theory is not possible even for this restricted class of systems. This follows from the results in [6] where DeLellis gave initial data for a class of symmetric, multi-d, commuting, nonlinear systems whose corresponding solutions suffer immediate blowup in BV. Furthermore, this can occur for data arbitrarily close to a constant. We are not aware of concrete examples of immediate BV-blowup, akin to DeLellis' examples, for nonlinear, non-commuting multi-d systems. Our second example mentioned above provides an example at the linear level.

Having used radial solutions to generate examples of BV instability for the 3-d linearized Euler system, we next provide a global existence result for such radial solutions. Our motivation is as follows. While standard arguments based on energy methods provide global existence for general, linear and symmetrizable systems, no such result is known for nonlinear systems. Even for the restricted class of radial solutions, global existence remains an open problem for the full Euler model (i.e., including energy conservation). Existence has been established for radial isentropic flows via arguments based on compensated compactness [3,4,15,20]; however, there is little hope of extending these results to the full model. It is therefore of interest to consider alternative construction schemes - even at the level of radial solutions to the linearized Euler model.

Our existence result for radial solutions of the 3-d linearized Euler system exploits a certain scaling of the dependent variables which yields a standard 1-d system without singular source terms. A 1-d front-tracking scheme, together with an application of Helly's selection theorem, yields global existence of the scaled solution. Finally, applying the inverse scalings we obtain, typically unbounded, global solutions to the original radial linearized Euler system in $\mathbb{R}^3$.

This approach highlights, admittedly in a simple setting, the feasibility of using "radial front-tracking" to establish existence of radially symmetric solutions. The key step is to identify a class of suitable building blocks, i.e., solutions generated by initial data that contain a single jump discontinuity. For this we use particularly simple, piecewise r-independent solutions; see Section 2.3. In addition to providing the relevant building blocks for radial front-tracking, these special solutions will also be used in one of the examples of BV-instability. Identifying suitable building blocks in the case of the nonlinear Euler system remains an outstanding challenge.

The rest of the paper is organized as follows. Section 2 gives the linearized 3-d Euler system, defines weak solutions, introduce the r-scaled system, and provides the relevant building blocks. Section 3 presents the examples of BV-instability and L^∞-blowup as discussed above. Finally, Section 4 gives the details of the radial front-tracking scheme, giving global existence of radial solutions for a rich class of finite-energy data (cf. Theorem 4.1).

2. Preliminaries

Consider the compressible Euler system for radial flow in $\mathbb{R}^3_{\mathbf{x}}$:

$$\rho_t + u\rho_r + \rho(u_r + \tfrac{2u}{r}) = 0 \tag{2.1}$$

$$\rho(u_t + uu_r) + p_r = 0 \tag{2.2}$$

Here $r = |\mathbf{x}| \geq 0$ is the radial distance to the origin, and $\rho = \rho(t,r)$, $u = u(t,r)$ denote the density and radial velocity of the fluid, respectively, so that the 3-d velocity field is $\mathbf{u}(t,\mathbf{x}) = u(t,r)\frac{\mathbf{x}}{r}$. The pressure $p = p(\rho)$ is assumed to be an increasing function of ρ.

We linearize (2.1)-(2.2) about $(\rho,u) \equiv (\bar\rho, 0)$ ($\bar\rho > 0$ constant). With

$$v := c\rho, \qquad w := \bar\rho u, \qquad c := \sqrt{p'(\bar\rho)},$$

we obtain the symmetric, linear system

$$\begin{bmatrix} v \\ w \end{bmatrix}_t + \begin{bmatrix} 0 & c \\ c & 0 \end{bmatrix} \begin{bmatrix} v \\ w \end{bmatrix}_r = \begin{bmatrix} -\frac{2c}{r} w \\ 0 \end{bmatrix}, \tag{2.3}$$

which is to be solved on $\mathbb{R}^+_t \times \mathbb{R}^+_r$ with initial data

$$v(0,r) = v_0(r) := c\rho_0(r), \qquad w(0,r) = w_0(r) := \bar\rho u_0(r). \tag{2.4}$$

2.1. Weak solutions. To define weak solutions of the radial system (2.3) we start from the multi-d, linearized Euler system

$$\rho_t + \bar\rho \operatorname{div}_{\mathbf{x}} \mathbf{u} = 0 \qquad \bar\rho \mathbf{u}_t + c^2 \operatorname{grad}_{\mathbf{x}} \rho = 0, \tag{2.5}$$

where ρ and $\mathbf{u} = (u_1,u_2,u_3)$ denote perturbations of the constant background state $(\bar\rho, 0)$. In terms of

$$v := c\rho, \qquad \mathbf{w} = (w_1,w_2,w_3) := \bar\rho \mathbf{u}, \tag{2.6}$$

the weak form requires that

$$\int_{\mathbb{R}^3} \theta_0 v_0 \, d\mathbf{x} + \int_{\mathbb{R}^+} \int_{\mathbb{R}^3} \theta_t v + c \operatorname{grad}_x \theta \cdot \mathbf{w} \, d\mathbf{x} dt = 0 \tag{2.7}$$

and

$$\int_{\mathbb{R}^3} \theta_0 w_{i0} \, d\mathbf{x} + \int_{\mathbb{R}^+} \int_{\mathbb{R}^3} \theta_t w_i + c\theta_{x_i} v \, d\mathbf{x} dt = 0 \quad (i = 1,2,3) \tag{2.8}$$

for all smooth and compactly supported test functions $\theta \in C_c^\infty(\mathbb{R}_t \times \mathbb{R}^3_x)$. Here and below we use a '0' subscript on a function of (t,r) to denote evaluation at time $t = 0$: $\theta_0(r) \equiv \theta(0,r)$, etc. Positing radial symmetry, i.e.,

$$v(t,\mathbf{x}) = v(t,r) \qquad \mathbf{w}(t,\mathbf{x}) = w(t,r)\tfrac{\mathbf{x}}{r},$$

and changing to spherical coordinates, we obtain the following (see [10] for details). Equation (2.7) yields

$$\int_{\mathbb{R}^+} \int_{\mathbb{R}^+} [v\varphi_t + cw\varphi_r] \, r^2 dr dt + \int_{\mathbb{R}^+} v_0(r)\varphi_0(r) r^2 dr = 0 \tag{2.9}$$

where

$$\varphi(t,r) = \int_{|x|=1} \theta(t,rx)\, dS_x,$$

while (2.8) yields

$$\int_{\mathbb{R}^+}\int_{\mathbb{R}^+} \left[w\psi_t + cv(\psi_r + \tfrac{2}{r}\psi)\right] r^2 dr dt + \int_{\mathbb{R}^+} w_0(r)\psi_0(r) r^2 dr = 0 \tag{2.10}$$

where

$$\psi(t,r) := \int_{|x|=1} x_i \theta(t,rx)\, dS_x.$$

Note that the "test function" $\varphi(t,r)$ in (2.9) typically does not vanish as $r\downarrow 0$, while $\psi(t,r)$ in (2.10) vanishes at a linear rate as $r\downarrow 0$. (In particular, the term $\frac{2}{r}\psi$ in (2.10) is bounded.) This motivates the following definitions.

Definition 2.1. *With $\mathbb{R}^+ \equiv (0,\infty)$ and $\mathbb{R}_0^+ \equiv [0,\infty)$, we introduce the following sets of functions. $C_c^\infty(\mathbb{R}\times\mathbb{R}_0^+)$ denotes the set of functions $\varphi(t,r)$ that are restrictions to $\mathbb{R}\times\mathbb{R}_0^+$ of smooth and compactly supported functions defined on $\mathbb{R}\times\mathbb{R}$. $C_0^\infty(\mathbb{R}\times\mathbb{R}_0^+)$ denotes the set of functions $\psi\in C_c^\infty(\mathbb{R}\times\mathbb{R}_0^+)$ with the additional property that $\lim_{r\downarrow 0}\psi(t,r)=0$ for all $t\geq 0$.*

Definition 2.2. *Consider the radial wave system (2.3) for $(t,r)\in\mathbb{R}_0^+\times\mathbb{R}_0^+$. For initial data $v_0,w_0\in L^1_{loc}(\mathbb{R}_0^+, r^2dr)$ we say that the function pair $v,w:\mathbb{R}_0^+\times\mathbb{R}_0^+\to\mathbb{R}$ is* a weak solution *of the corresponding initial value problem for the wave system (2.3) provided:*

(i) *the solution maps $t\mapsto v(t)$ and $t\mapsto w(t)$ map $\mathbb{R}_0^+$ continuously into $L^1_{loc}(\mathbb{R}_0^+, r^2dr)$ with $v(0)=v_0$ and $w(0)=w_0$; and*

(ii) *the equations in (2.3) are satisfied in the following distributional senses: (2.9) is satisfied for all $\varphi\in C_c^\infty(\mathbb{R}\times\mathbb{R}_0^+)$, and (2.10) is satisfied for all $\psi\in C_0^\infty(\mathbb{R}\times\mathbb{R}_0^+)$.*

2.2. Scaled variables; AB-system. It will be convenient to employ the following r-weighted variables:

$$A(t,r) := rv(t,r), \qquad B(t,r) := r^2 w(t,r). \tag{2.11}$$

This transforms the system (2.3) into

$$rA_t + cB_r = 0, \qquad B_t + crA_r = cA, \tag{2.12}$$

or, in conservative form,

$$(rA)_t + cB_r = 0 \tag{2.13}$$

$$B_t + c(rA)_r = 2cA, \tag{2.14}$$

for $(t,r)\in\mathbb{R}^+\times\mathbb{R}^+$. We refer to either form as the *AB-system.*

Reformulating Definition 2.2 in terms of the rescaled unknowns A and B yields the following definition for the AB-system. (Recall Definition 2.1.)

Definition 2.3. *Consider the AB-system (2.13)-(2.14) in conservative form. For initial data $A_0,B_0\in L^1_{loc}(\mathbb{R}_0^+, dr)$ we say that the function pair $A,B:\mathbb{R}^+\times\mathbb{R}^+\to\mathbb{R}$ is a* weak solution *of the corresponding initial value problem for the AB-system provided:*

(i) *the solution maps* $t \mapsto A(t)$ *and* $t \mapsto B(t)$ *map* $\mathbb{R}_0^+$ *continuously into* $L^1_{loc}(\mathbb{R}_0^+, dr)$ *with* $A(0) = A_0$ *and* $B(0) = B_0$*; and*

(ii) (2.13)-(2.14) *are satisfied in the following distributional sense:*

$$\int_{\mathbb{R}^+}\int_{\mathbb{R}^+} rA\varphi_t + cB\varphi_r \, dr dt + \int_{\mathbb{R}^+} rA_0(r)\varphi_0(r)\, dr = 0 \tag{2.15}$$

for all $\varphi \in C_c^\infty(\mathbb{R}\times\mathbb{R}_0^+)$*, and*

$$\int_{\mathbb{R}^+}\int_{\mathbb{R}^+} B\psi_t + cA(r\psi_r + 2\psi)\, dr dt + \int_{\mathbb{R}^+} B_0(r)\psi_0(r)\, dr = 0 \tag{2.16}$$

for all $\psi \in C_0^\infty(\mathbb{R}\times\mathbb{R}_0^+)$*.*

We do not impose a boundary condition along $\{r = 0\}$. However, we shall restrict attention to finite energy solutions, i.e., we require that

$$E(t) := \tfrac{1}{2}\int_0^\infty \big[w^2(t,r) + v^2(t,r)\big] r^2\, dr \equiv \tfrac{1}{2}\int_0^\infty A(t,r)^2 + \tfrac{B(t,r)^2}{r^2}\, dr \tag{2.17}$$

is finite (and in fact constant) for all times $t \geq 0$. It will follow from this that the approximate solutions to the AB-system we construct below will vanish near $r = 0$ (see Section 2.3.3).

2.3. Elementary solutions to the AB-system. We make use of a family of particularly simple solutions to the AB-system. These will be used both for examples of BV-instability (Section 3) and as building blocks for constructing approximate front-tracking solutions (Section 4). It is immediate to verify that

$$\begin{bmatrix} A(t,r) \\ B(t,r) \end{bmatrix} := \begin{bmatrix} a \\ act + b \end{bmatrix} \tag{2.18}$$

is an exact solution to the AB-system for any choice of constants $a, b \in \mathbb{R}$. We proceed to verify that they, together with their t-translates, provide an invariant family of piecewise-constant-in-r solutions. For this we need to resolve initial Riemann problems, interaction Riemann problems, and also boundary Riemann problems along $r = 0$. The system (2.13)-(2.14) has constant characteristic speeds $\pm c$, with Rankine-Hugoniot relations

$$[\![B]\!] = \pm[\![rA]\!] \quad \text{across discontinuities with speed } \pm c\text{, respectively.} \tag{2.19}$$

2.3.1. Initial Riemann problems. Consider an initial Riemann problem for the AB-system (2.13)-(2.14), centered at $r = \bar{r} > 0$, and with constant left and right states

$$\begin{bmatrix} a_- \\ b_- \end{bmatrix} \qquad \text{and} \qquad \begin{bmatrix} a_+ \\ b_+ \end{bmatrix},$$

respectively. The solution consists of three parts separated by discontinuities propagating along the two straight lines $r = \bar{r} \pm ct$. The leftmost and rightmost parts of the solution are, according to (2.18), given by

$$\begin{bmatrix} a_- \\ a_-ct + b_- \end{bmatrix} \qquad \text{and} \qquad \begin{bmatrix} a_+ \\ a_+ct + b_+ \end{bmatrix},$$

respectively, while (2.19) shows that the emerging middle state is

$$\begin{bmatrix} \hat{a} \\ \hat{a}ct+\hat{b} \end{bmatrix}, \tag{2.20}$$

with

$$\hat{a}=\langle a\rangle-\tfrac{1}{2\bar{r}}[[b]], \qquad \text{and} \qquad \hat{b}=\langle b\rangle-\tfrac{\bar{r}}{2}[[a]], \tag{2.21}$$

where we have used the notations

$$\langle a\rangle:=\tfrac{1}{2}(a_+ + a_-) \qquad \text{and} \qquad [[a]]:=a_+ - a_-, \tag{2.22}$$

and similarly for $\langle b\rangle$ and $[[b]]$.

2.3.2. Wave interactions in $\{t>0, r>0\}$. Consider two discontinuities propagating along $r=\bar{r}\pm c(t-\bar{t})$, respectively, that meet at $(\bar{t},\bar{r})$, where $\bar{t}>0$ and $\bar{r}>0$. Denoting the incoming left, middle, and right states by

$$\begin{bmatrix} a_- \\ a_-ct+b_- \end{bmatrix}, \qquad \begin{bmatrix} a_0 \\ a_0ct+b_0 \end{bmatrix}, \qquad \text{and} \qquad \begin{bmatrix} a_+ \\ a_+ct+b_+ \end{bmatrix},$$

respectively, the Rankine-Hugoniot relations (2.19) yield

$$(b_0+a_0ct)-(b_-+a_-ct)=(c(t-\bar{t})+\bar{r})(a_0-a_-) \tag{2.23}$$
$$(b_++a_+ct)-(b_0+a_0ct)=(c(t-\bar{t})-\bar{r})(a_+-a_0). \tag{2.24}$$

Adding these two identities and solving for $[[b]]\equiv b_+-b_-$ gives

$$[[b]]=2\bar{r}(a_0-\langle a\rangle)-[[a]]c\bar{t}, \tag{2.25}$$

with the same notation as in (2.22). Next, denoting the outgoing middle state as in (2.20), the Rankine-Hugoniot relations (2.19) yield

$$(\hat{b}+\hat{a}ct)-(b_-+a_-ct)=(c(t-\bar{t})-\bar{r})(\hat{a}-a_-) \tag{2.26}$$
$$(b_++a_+ct)-(\hat{b}+\hat{a}ct)=(c(t-\bar{t})+\bar{r})(a_+-\hat{a}). \tag{2.27}$$

Adding the last two identities and solving for $\hat{a}$ gives

$$\hat{a}=\langle a\rangle-\tfrac{1}{2\bar{r}}\left([[b]]+[[a]]c\bar{t}\right), \tag{2.28}$$

again with the same notation as in (2.22). According to (2.25) this yields

$$\hat{a}=a_++a_--a_0. \tag{2.29}$$

(The explicit expression for $\hat{b}$ will not be needed.)

2.3.3. Riemann problem at the origin; wave reflection along $\{t>0, r=0\}$. Finally we need to analyze the situation along $\{r=0\}$. Consider first the situation at time $t=0$, where we use piecewise constant approximations to the initial data $A_0(r)$ and $B_0(r)$. Let b_0 be the constant value used to approximate $B_0(r)$ near $r=0$. From the requirement of finite energy it follows that $b_0=0$ (see (2.17)). We thus have an initial state of the form

$$\begin{bmatrix} a_0 \\ 0 \end{bmatrix} \qquad \text{near } r=0 \text{ at time } t=0.$$

The boundary Riemann problem at $(t,r)=(0,0)$ must give a single discontinuity along $\{r=ct\}$. The solution to its right is given by (2.18):

$$\begin{bmatrix} A(t,r) \\ B(t,r) \end{bmatrix} = \begin{bmatrix} a_0 \\ a_0ct \end{bmatrix} \qquad \text{for } r>ct,$$

which is to connect to a state, again of the form (2.18), on its left. It follows from the Rankine-Hugoniot condition, together with the requirement of finite energy, that the left state is trivial

$$\begin{bmatrix} A(t,r) \\ B(t,r) \end{bmatrix} \equiv \begin{bmatrix} 0 \\ 0 \end{bmatrix} \qquad \text{for } 0<r<ct.$$

It remains to consider the case when a left-moving discontinuity, along $r=\bar{r}-ct$, say, and with the trivial state on its left, meets the boundary $r=0$ at time $\bar{t}:=\frac{\bar{r}}{c}$. Letting the state to the right of the discontinuity be

$$\begin{bmatrix} A(t,r) \\ B(t,r) \end{bmatrix} = \begin{bmatrix} \tilde{a} \\ \tilde{b}+\tilde{a}ct \end{bmatrix} \qquad (r>\bar{r}-ct, t<\bar{t}), \tag{2.30}$$

the Rankine-Hugoniot relation (2.19) for a left-moving discontinuity gives

$$\tilde{b}+\tilde{a}\bar{r}=0. \tag{2.31}$$

The left-moving wave will reflect off $r=0$ at time $\bar{t}$ as a right-moving discontinuity along $r=ct-\bar{r}$. Imposing finite energy as above, we use the trivial state $(A,B)=(0,0)$ for $0<r<ct-\bar{r}$. It is immediate to verify that, thanks to (2.31), the Rankine-Hugoniot condition is then verified across the reflected discontinuity. Note that, as the energy (2.17) is finite, and since the characteristic rectangle on which (2.30) holds meets the boundary $\{r=0\}$ at $t=\bar{t}$, it follows that $B(t,r)=\tilde{b}+\tilde{a}ct$ must vanish for $t=\bar{t}=\frac{\bar{r}}{c}$; again, this holds thanks to (2.31). Thus, by imposing finite energy we ensure that solutions to the AB-system with piecewise constant initial data vanish on a band of adjacent triangles bounded by characteristic lines and $\{r=0\}$.

The above calculations confirm that the family of solutions (2.18) (and their t-translates) provide a family of piecewise-constant-in-r solutions to (2.13)-(2.14) that is invariant under resolution of Riemann problems. They will be used in Section 4 to build front-tracking approximations for (2.3).

3. BV-instability for 3-d linearized radial Euler

In this section we employ radial solutions to study BV-instability for the linearized Euler system in $\mathbb{R}^3$ (see (2.5)-(2.6))

$$v_t + c\,\mathrm{div}_{\mathbf{x}}\mathbf{w} = 0 \qquad \mathbf{w}_t + c\,\mathrm{grad}_{\mathbf{x}} v = 0, \tag{3.1}$$

whose radial solutions $(v,\mathbf{w})=(v(t,r),w(t,r)\frac{\mathbf{x}}{|\mathbf{x}|})$ solve (2.3).

A *radial Riemann problem* for (3.1) at $r=\bar{r}$ refers to an initial value problem whose data $(v_0,\mathbf{w}_0=w_0\frac{\mathbf{x}}{|\mathbf{x}|})$ are such that v_0 and w_0 are piecewise constant with a single jump discontinuity across the sphere of radius $\bar{r}>0$.

We fix a large radius R and restrict attention to the solutions within the ball B_R of radius R about the origin. By finite speed of propagation it is clear that we can alter the initial data outside B_R to obtain data of compact support whose solutions exhibit the same type of local behavior near the origin. In calculating the two parts of the

BV-norm (L^1-norm + variation) we drop the geometric factor 4π throughout. Also, we write $X \sim Y$ ($X \lesssim Y$) when $X = C\cdot Y$ ($X \leq C\cdot Y$, respectively) for a constant $C<\infty$. Finally, we abuse notation slightly by using the same symbol for a radial function whether regarded as a function of (t,r) or of $(t,\mathbf{x})$. (However, we stress that all norms we calculate in this section are norms of functions defined on $\mathbb{R}^3_{\mathbf{x}}$.)

3.1. Amplitude blowup without BV-blowup. Consider a single radial Riemann problem for (3.1) with initial data

$$\begin{bmatrix} v_0(r) \\ w_0(r) \end{bmatrix} = \begin{cases} \begin{bmatrix} v_- \\ 0 \end{bmatrix} & 0<r<\bar{r} \\ \begin{bmatrix} v_+ \\ 0 \end{bmatrix} & r>\bar{r}, \end{cases} \tag{3.2}$$

for different constants $v_\pm$.

REMARK 3.1. As discussed above, the data are understood to be truncated to vanish far from the origin, and attention is restricted to the behavior of the solution within a large ball B_R about the origin. At any time $t>0$, the contribution from $r>R$ to the various norms we compute is bounded, and it is therefore not calculated in detail.

The data (3.2) generate two discontinuities along the characteristics $r=\bar{r}+ct$ and $r=\bar{r}-ct$, with the latter being reflected into $r=ct-\bar{r}$ at time $\bar{t}:=\frac{\bar{r}}{c}$. Note that no discontinuity is generated at the origin at time zero. The solution is explicitly given by (see Figures 3.1 and 3.2):

$$\begin{bmatrix} v(t,r) \\ w(t,r) \end{bmatrix} = \begin{cases} \begin{bmatrix} v_- \\ 0 \end{bmatrix} & \text{for } (t,r)\in\Omega_1 \\ \begin{bmatrix} \langle v\rangle_0 + \frac{ct}{2r}[\![v]\!]_0 \\ \frac{[\![v]\!]_0}{4}\left(\frac{(ct)^2-r^2-\bar{r}^2}{r^2}\right) \end{bmatrix} & \text{for } (t,r)\in\Omega_2 \\ \begin{bmatrix} v_+ \\ 0 \end{bmatrix} & \text{for } (t,r)\in\Omega_3, \end{cases} \tag{3.3}$$

where $\langle v\rangle_0 = \frac{1}{2}(v_+ + v_-)$, $[\![v]\!]_0 = v_+ - v_-$, and

$$\Omega_1 = \{(t,r)\,|\,0<r<\bar{r}-ct \text{ and } t<\bar{t}\}$$

$$\Omega_2 = \{(t,r)\,|\,ct-\bar{r}<r<ct+\bar{r} \text{ and } r>\bar{r}-ct\}$$

$$\Omega_3 = \{(t,r)\,|\,0<r<ct-\bar{r} \text{ and } t>\bar{t}, \text{ or } r>\bar{r}+ct\}.$$

A direct calculation verifies that the expressions in (3.3) define classic solutions of (2.3) within each of Ω_1-Ω_3, and that the Rankine-Hugoniot relations $[\![w]\!] = \pm[\![v]\!]$ across characteristics with speeds $\pm c$, respectively, are also met. It follows that the corresponding solution of (3.1)-(3.2) is $(v(t,r), w(t,r)\frac{\mathbf{x}}{|\mathbf{x}|})$ where v and w are given by (3.3).

Clearly, the initial data (v_0,w_0) are bounded and of (locally) finite energy, and with $\|v_0,w_0\|_{BV(B_R)}<\infty$.

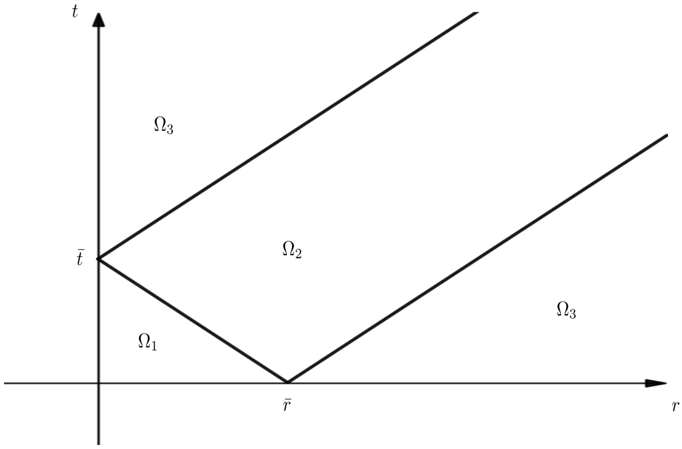

FIG. 3.1. *Regions related to the solution* (3.3).

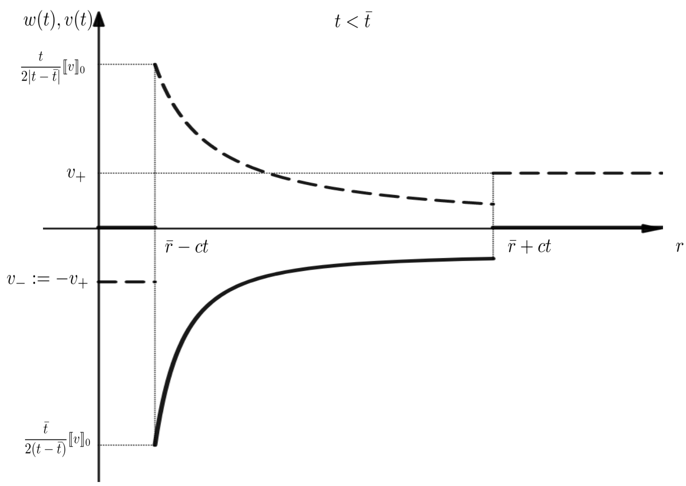

FIG. 3.2. *v-component (dashed) and w-component (solid) of the solution* (3.3) *at a time* $t \in (0,\bar{t})$, *in the particular case with* $v_- = -v_+ < 0$.

Next, evaluating $(v(t,r),w(t,r))$ along the focusing characteristic $r = (\bar{r} - ct)+$, for $t < \bar{t}$, yields

$$v(t,(\bar{r}-ct)+) = \langle v \rangle_0 + \tfrac{[[v]]_0}{2} \tfrac{t}{\bar{t}-t}$$

and

$$w(t,(\bar{r}-ct)+) = \tfrac{[[v]]_0}{2} \tfrac{\bar{t}}{t-\bar{t}}.$$

These expressions show that both v and w suffer L^∞-blowup as $t\uparrow\bar t$.

We proceed to verify that $\|v(t)\|_{BV(B_R)}$ and $\|w(t)\|_{BV(B_R)}$ remain bounded for all $t>0$. In the following calculations we use that for a radial function $f(\mathbf{x})=f(|\mathbf{x}|)$ on $\mathbb{R}^3$:

- a jump discontinuity across $|\mathbf{x}|=r$ contributes $\sim r^2|[\![f]\!]_r|$ to its variation;
- if f is smooth for $r_-<|\mathbf{x}|<r_+$, its variation over this region is

$$\sim\int_{r_-}^{r_+}|f'(r)|r^2\,dr;$$

see Section 13.1 in [16]. First, consider times $0<t\le\bar t$. As $v(t,\cdot)$ suffers jumps across $r=\bar r\pm ct$, we obtain from (3.3) that (with $R>2\bar r$)

$$\begin{aligned}
&\|v(t)\|_{BV(B_R)}=\|v(t)\|_{L^1(B_R)}+\mathrm{Var}_{B_R}v(t)\\
&\lesssim\int_0^{\bar r-ct}|v_-|r^2\,dr+\int_{\bar r-ct}^{\bar r+ct}|v(t,r)|r^2\,dr+\int_{\bar r+ct}^{R}|v_+|r^2\,dr\\
&\quad+(\bar r-ct)^2|[\![v(t)]\!]_{\bar r-ct}|+(\bar r+ct)^2|[\![v(t)]\!]_{\bar r+ct}|+\int_{\bar r-ct}^{\bar r+ct}|v_r(t,r)|r^2\,dr\\
&\le\tfrac{|v_-|}{3}(\bar r-ct)^3+\tfrac{|v_+|}{3}(R^3-(\bar r+ct)^3)\\
&\quad+\tfrac{|\langle v\rangle_0|}{3}((\bar r+ct)^3-(\bar r-ct)^3)+c^2(t^2+\bar t^2)|[\![v]\!]_0|,
\end{aligned}$$

which remains uniformly bounded for $0<t\le\bar t$. Similarly, since $w(t,\cdot)$ suffers jumps across $r=\bar r\pm ct$ and vanishes on $(0,\bar r-ct)$ and on $(\bar r+ct,\infty)$, we have (for $R>2\bar r$ and $0<t\le\bar t$)

$$\begin{aligned}
\|w(t)\|_{BV(B_R)}&=\|w(t)\|_{L^1(B_R)}+\mathrm{Var}_{B_R}w(t)\\
&\lesssim\int_{\bar r-ct}^{\bar r+ct}|w(t,r)|r^2dr+(\bar r-ct)^2|[\![w(t)]\!]_{\bar r-ct}|\\
&\quad+(\bar r+ct)^2|[\![w(t)]\!]_{\bar r+ct}|+\int_{\bar r-ct}^{\bar r+ct}|w_r(t,r)|r^2dr\\
&=|[\![v]\!]_0|\left[ct(\bar r^2-\tfrac13(ct)^2)+\bar r^2+\tfrac{(\bar r^2-(ct)^2)}{2}\cdot\log\tfrac{\bar r+ct}{\bar r-ct}\right],
\end{aligned}$$

which again remains uniformly bounded for $0<t\le\bar t$.

Entirely similar calculations show that $\|v(t)\|_{BV(B_R)}$ and $\|w(t)\|_{BV(B_R)}$ are bounded at all times $t>\bar t$ as well.

Finally, we translate these results into statements about solutions to the 3-d linearized Euler system (3.1). The calculations above show that the corresponding solution $(v,\mathbf{w})=(v,w_1,w_2,w_3)$ of (3.1) suffers blowup in $L^\infty(B_R)$ as $t\uparrow\bar t$, while $\|v(t)\|_{BV(B_R)}$ and $\|w_i(t)\|_{L^1(B_R)}$ $(i=1,2,3)$ remain bounded for all times. Also, since

$$|\partial_{x_j}w_i|\lesssim|w_r|+\tfrac{|w|}{r},\tag{3.4}$$

we deduce from above that $\mathrm{Var}_{B_R}w_i(t)$ remains bounded provided

$$\int_{\bar r-ct}^{\bar r+ct}|w(t,r)|r\,dr\qquad\text{remains bounded.}$$

A direct calculation shows that the latter integral is bounded (up to a constant) by $\bar rct+(\bar r^2-(ct)^2)\cdot\log\left|\frac{\bar r+ct}{\bar r-ct}\right|$ for all times $0<t\le\bar t$.

A similar calculation yields the same result for $t > \bar{t}$, and we conclude that each $w_i(t)$, $i = 1,2,3$, remains bounded in $BV(B_R)$ for all times.

Summing up, we have that the radial Riemann problem with data (3.2) for the 3-d linearized Euler system (3.1) generates a solution that remains uniformly bounded in $BV(B_R)$ for all times, while suffering blowup in $L^\infty(B_R)$ due to wave-focusing at time $t = \bar{t}$.

3.2. BV-instability without wave focusing and from small data. For our second example we consider a radial solution of (3.1) generated by initial data that suffer jump discontinuities across an infinite sequence of diminishing radii.

We want the solution to contain only outgoing waves. It is then convenient to prescribe initial data $(v_0(r), w_0(r))$ with the property that $r \mapsto (A_0(r), B_0(r)) := (rv_0(r), r^2 w_0(r))$ is piecewise constant, and to use the analysis in Section 2.3.1 to make sure that no focusing wave (i.e., no wave with speed $-c$) is generated. It follows from (2.20)-(2.21) that, for the AB-system (2.13)-(2.14), the Riemann problem at $r = \bar{r}$ with inner and outer states $[a_-, b_-]$ and $[a_+, b_+]$, respectively, produces no focusing wave if and only if

$$[[b]]_{\bar{r}} = \bar{r}[[a]]_{\bar{r}} \qquad \text{(no focusing wave)}, \tag{3.5}$$

where $[[\cdot]]_{\bar{r}}$ denotes jump across $r = \bar{r}$.

We further want a situation where the initial data are arbitrarily small in L^∞ and BV, while the resulting solution suffers immediate blowup in BV. (This behavior is motivated by DeLellis' examples in [6]; see Section 1.)

We start by fixing an integer $N > 1$ which will serve as index for a sequence of initial data $(v_0^N(r), w_0^N(r))$ with the required properties. For convenience we mostly drop the N from the notation. To define the data we introduce the following notations. For integer $k \geq 0$ we set

$$\sigma_k := \begin{cases} 0 & k \text{ even} \\ -1 & k \text{ odd,} \end{cases}$$

and

$$\beta_k := \tfrac{1}{(N+k+\sigma_k)\sqrt{N+k}}.$$

It is immediate to verify that (β_k) is a strictly decreasing sequence of positive numbers. We define

$$a_N := 0, \qquad b_N := \sum_{k=0}^{\infty} (-1)^{k+1} \beta_k, \tag{3.6}$$

and for $n \geq N+1$ set

$$a_n := \begin{cases} 0 & n-N \text{ even} \\ \frac{1}{n-1} & n-N \text{ odd} \end{cases}, \tag{3.7}$$

and

$$b_n := b_N - \sum_{k=0}^{n-N-1} (-1)^{k+1} \beta_k = \sum_{k=n-N}^{\infty} (-1)^{k+1} \beta_k. \tag{3.8}$$

We finally set

$$r_n := \frac{1}{\sqrt{n}}$$

and define the N-th set of initial data for the (A,B)-system as follows:

$$A_0(r) := \begin{cases} a_N = 0 & r > r_N \\ a_n & r_n < r < r_{n-1}, n \geq N+1, \end{cases}$$

and

$$B_0(r) := \begin{cases} b_N & r > r_N \\ b_n & r_n < r < r_{n-1}, n \geq N+1. \end{cases}$$

It is readily verified that these initial data are such that (3.5) is satisfied across each radius $r = r_n$. The corresponding initial data for v and w are

$$v_0(r) = \tfrac{A_0(r)}{r}, \qquad w_0(r) = \tfrac{B_0(r)}{r^2}. \tag{3.9}$$

It follows that the resulting solution of (3.1) contains no focusing waves.

We next estimate the L^∞- and BV-norms of $v_0(r)$ and $w_0(r)$. As in the previous example it suffices to consider the behavior on a bounded set which we fix as the unit ball $B_1 \subset \mathbb{R}^3$. We have

$$\begin{aligned} \|v_0(r)\|_{L^\infty(B_1)} &= \sup_{\substack{n\geq N \\ n-N\,\text{odd}}} \sup_{r_n<r<r_{n-1}} \left|\tfrac{a_n}{r}\right| = \sup_{\substack{n\geq N \\ n-N\,\text{odd}}} \tfrac{a_n}{r_n} \\ &\leq \sup_{n\geq N} \tfrac{\sqrt{n}}{n-1} = \tfrac{\sqrt{N}}{N-1}, \end{aligned} \tag{3.10}$$

and (with $r_{N-1} := 1$)

$$\begin{aligned} \|w_0(r)\|_{L^\infty(B_1)} &= \sup_{n\geq N} \sup_{r_n<r<r_{n-1}} \left|\tfrac{b_n}{r^2}\right| = \sup_{n\geq N} \tfrac{|b_n|}{r_n^2} = \sup\nolimits_{n\geq N} n|b_n| \\ &= \sup_{n\geq N} n\left| \sum_{k=n-N}^{\infty} (-1)^{k+1}\beta_k \right| \leq \sup_{n\geq N} n|\beta_{n-N}| \\ &\leq \sup_{n\geq N} \tfrac{n}{(n+\sigma_n)\sqrt{n}} \leq \sup\nolimits_{n\geq N} \tfrac{\sqrt{n}}{n-1} = \tfrac{\sqrt{N}}{N-1}, \end{aligned} \tag{3.11}$$

where, in (3.11), we used that the tail of an alternating series with decreasing terms is bounded by the size of the first term of the tail. It follows from (3.10)-(3.11) that the $L^\infty(B_1)$-norm, and thus the $L^1(B_1)$- and $L^2(B_1)$-norms, of the data $(v_0(r), w_0(r)) \equiv (v_0^N(r), w_0^N(r))$ tend to zero as $N \to \infty$.

Next consider the variations of $v_0(r)$ and $w_0(r)$. We have

$$\begin{aligned} \mathrm{Var}_{B_1} v_0 &\lesssim \sum_{n\geq N} r_n^2 |[[v_0]]_{r_n}| + \sum_{\substack{n\geq N \\ n-N\,\text{even}}} \int_{r_{n+1}}^{r_n} \left| \left(\tfrac{a_{n+1}}{r}\right)_r \right| r^2\, dr \\ &\lesssim \sum_{n\geq N} \tfrac{1}{n\sqrt{n}} + \sum_{n\geq N} \tfrac{1}{n} \left(\tfrac{1}{\sqrt{n}} - \tfrac{1}{\sqrt{n+1}} \right), \end{aligned} \tag{3.12}$$

and

$$\begin{aligned}\mathrm{Var}_{B_1} w_0 &\lesssim \sum_{n\geq N} r_n^2 |[[w_0]]_{r_n}| + \sum_{n\geq N} \int_{r_{n+1}}^{r_n} \left|\left(\tfrac{b_{n+1}}{r^2}\right)_r\right| r^2\,dr \\ &\lesssim \sum_{n\geq N} |b_{n+1}-b_n| + \sum_{n\geq N} |b_{n+1}| \log \tfrac{r_n}{r_{n+1}} \\ &\lesssim \sum_{n\geq N} |\beta_{n-N}| + \sum_{n\geq N} \left| \sum_{k=n-N}^{\infty} (-1)^{k+1}\beta_k \right| \log \tfrac{n+1}{n} \\ &\leq \sum_{n\geq N} |\beta_{n-N}| + \sum_{n\geq N} |\beta_{n-N}| \log \tfrac{n+1}{n} \lesssim \sum_{n\geq N} \tfrac{1}{(n-1)\sqrt{n}}. \end{aligned} \tag{3.13}$$

It follows from (3.12)-(3.13) that the variations of both $v_0(r) \equiv v_0^N(r)$ and $w_0(r) \equiv w_0^N(r)$ on B_1 tend to zero as $N \to \infty$. As the same applies to their $L^1(B_1)$-norms, we conclude that the BV($\mathbb{R}^3$)-norm of the initial data can be made arbitrarily small by choosing N sufficiently large. By using (3.4) as in Section 3.1 we obtain that the same conclusion holds for the corresponding initial data $(v_0^N(r), \mathbf{w}_0^N(r))$ for the linearized Euler system (3.1).

We finally show that the corresponding solution suffers immediate blowup in BV, i.e. $(v(t,r),w(t,r)) \equiv (v_N(t,r),w_N(t,r))$ has infinite BV($\mathbb{R}^3$)-norm at all strictly positive times. For this it suffices to verify that the variation of $v(t,r)$ is unbounded whenever $t>0$. According to the calculations in Section 2.3.1, $v(t,r) = \frac{a_n}{r}$ within each of the strips $\{(t,r) : r_n + ct < r < r_{n-1} + ct\}$. With $[[a]]_n = a_{n+1} - a_n$ we therefore have

$$\mathrm{Var}_{B_1} v(t) \gtrsim \sum_{n\geq N} (r_n + ct)^2 \left| \tfrac{[[a]]_n}{r_n + ct} \right| > ct \sum_{n\geq N} \tfrac{1}{n} = \infty,$$

whenever $t>0$.

Summing up, this example provides finite-energy radial solutions of the 3-d linearized Euler system (3.1) whose initial data are arbitrarily small in $L^\infty(B_1)$ and $BV(B_1)$, and which generate only outgoing waves, while suffering immediate blowup in $BV(B_1)$.

4. Front tracking for the 3-d linearized radial Euler system

In this section we give a detailed proof of existence for the 3-d linearized radial Euler system (2.3). The approach exploits a 1-d front-tracking scheme for the rescaled variables $A = rv$ and $B = r^2 w$ introduced in Section 2.2. (See [2, 5, 11] for background on front tracking.)

The analysis in Section 2.3 shows how piecewise constant data (A_0, B_0) for the AB-system can be propagated for all times by resolving Riemann problems. We claim that these are exact weak solutions according to Definition 2.3. Part (i) of the definition will follow from the L^1-estimates in Section 4.3. For Part (ii) we first note that the front tracking solutions are, by construction, piecewise exact classical solutions. Also, all Riemann problems are resolved exactly according to the Rankine-Hugoniot relations (2.19). Finally, in verifying the weak form via integration by parts, the boundary terms $B\varphi|_{r=0}$ and $rA\psi|_{r=0}$ appear (in (2.13) and (2.14), respectively); both of these vanish since $A(t,0) = B(t,0) \equiv 0$ by construction.

To extract a convergent (sub)sequence of approximate solutions we shall apply Helly's criterion for BV-compactness in 1-d, and this requires bounding the variations of $A(t,r)$ and $B(t,r)$. Translated back to the original v and w variables, this will entail certain r-weighted variation bounds on the initial data v_0 and w_0. These bounds dictate the class of initial data covered by our approach.

The relevant variation and continuity estimates are given in Sections 4.1 and 4.3, respectively; Section 4.2 describes the approximation of initial data. A standard convergence argument then yields existence of weak solutions to (2.3); see Theorem 4.1.

4.1. Variation estimates. The first step is to monitor the spatial variation of solutions $A(t,r)$ and $B(t,r)$ to (2.13)-(2.14) that are piecewise constant and piecewise affine in t, respectively. We use the following notation: for any $f:\mathbb{R}_0^+\to\mathbb{R}$,

$$\operatorname{Var} f := \sup \sum_{i=1}^{N} |f(r_i) - f(r_{i-1})|,$$

where the supremum is taken over all finite, increasing selections of points in $\mathbb{R}^+$: $0 = r_0 < \cdots < r_N < \infty$.

4.1.1. Initial change in variations. Let A_0, B_0 be piecewise constant data with vanishing B-value near $r=0$ and jumps at $0<r_1<\cdots<r_N$. Let

$$A_0(r) = \sum_{i=0}^{N} a_i \chi_{[r_i,r_{i+1})}(r), \qquad B_0(r) = \sum_{i=1}^{N} b_i \chi_{[r_i,r_{i+1})}(r), \tag{4.1}$$

where $r_0=0$, $r_{N+1}=+\infty$, and we assume right-continuity. The data define a boundary Riemann problem at $r=0$, and a Riemann problem at each location $r=r_i$, $1\le i\le N$. With $b_0:=0$ the initial variations are

$$\operatorname{Var} A_0 = \sum_{i=1}^{N} |[\![a]\!]_i|, \qquad \operatorname{Var} B_0 = \sum_{i=1}^{N} |[\![b]\!]_i|, \tag{4.2}$$

where

$$[\![a]\!]_i := a_i - a_{i-1}, \qquad [\![b]\!]_i := b_i - b_{i-1} \qquad \text{for } 1\le i\le N.$$

Fix a time $t_0>0$ prior to any interaction of waves resulting from these Riemann problems. To calculate the variations of $r\mapsto A(t_0,r)$ and $r\mapsto B(t_0,r)$ we use the results from Sections 2.3.1 and 2.3.3. Recall that the requirement of finite energy implies that the boundary Riemann problem at $r=0$ is resolved by having the trivial state on the left connect to the state $(A,B)=(a_0,a_0ct)$ on the right across the characteristic line $r=ct$. This wave thus contributes $|a_0|$ to $\operatorname{Var} A(t_0)$ and $|a_0|ct_0$ to $\operatorname{Var} B(t_0)$. Next, let the outgoing middle state from the Riemann problem centered at $r=r_i$ $(1\le i\le N)$ be $(\hat a_i, \hat b_i + \hat a_i ct)$. From (2.21)-(2.22) it follows that the contribution to $\operatorname{Var} A(t_0)$ and $\operatorname{Var} B(t_0)$ from the two waves in the solution of this Riemann problem are given as

$$|a_i-\hat a_i| + |\hat a_i - a_{i-1}| = \tfrac12 |[\![a]\!]_i + \tfrac1r [\![b]\!]_i| + \tfrac12 |[\![a]\!]_i - \tfrac1r [\![b]\!]_i| \le |[\![a]\!]_i| + \tfrac{1}{r_i}|[\![b]\!]_i|,$$

and

$$\begin{aligned}&|(b_i + a_i ct_0) - (\hat b_i + \hat a_i ct_0)| + |(\hat b_i + \hat a_i ct_0) - (b_{i-1} + a_{i-1} ct_0)|\\ &\le (|[\![b]\!]_i| + r_i |[\![a]\!]_i|) + (|[\![a]\!]_i| + \tfrac{1}{r_i}|[\![b]\!]_i|)ct_0,\end{aligned}$$

respectively. We therefore have

$$\operatorname{Var} A(t_0) \leq \operatorname{Var} A_0 + |a_0| + \sum_{i=1}^{N} \tfrac{1}{r_i} |[[b]]_i| =: V(A_0, B_0), \tag{4.3}$$

and

$$\begin{aligned}\operatorname{Var} B(t_0) &\leq \big(\operatorname{Var} B_0 + \sum_{i=1}^{N} r_i |[[a]]_i|\big) + ct_0 \big(\operatorname{Var} A_0 + |a_0| + \sum_{i=1}^{N} \tfrac{1}{r_i} |[[b]]_i|\big) \\ &=: W(A_0, B_0) + ct_0 V(A_0, B_0). \end{aligned}\tag{4.4}$$

4.1.2. No change in variations across interactions. Consider the reflection of a left-moving characteristic into a right-moving characteristic at a time $\bar{t} > 0$ along $\{r = 0\}$. As the state adjacent to the boundary remains the same (trivial) state, the reflection does not change the variation of (A, B).

Next, consider the situation in Section 2.3.2 where two discontinuities with speeds $\pm c$ intersect at some point $(\bar{t}, \bar{r})$, with $\bar{t} > 0$ and $\bar{r} > 0$. With the same notation as there, the contribution to $\operatorname{Var} A(t)$ from the two approaching waves, before interaction and after interaction, respectively, are

$$|a_0 - a_-| + |a_+ - a_0| \qquad \text{and} \qquad |\hat{a} - a_-| + |a_+ - \hat{a}|.$$

According to (2.29), these two sums are identical, and the interaction contributes no change in the variation of A. Finally, it follows from this together with the Rankine-Hugoniot relations (2.19), that the interaction also contributes no change in the variation of B.

4.1.3. Changes in variations between interactions. Consider the situation between two consecutive interactions. With $A(t,r)$ and $B(t,r)$ piecewise constant and piecewise affine in t, respectively, assume $\bar{t} > 0$ and $\Delta t > 0$ are such that no discontinuities in $(A(t,r), B(t,r))$ meet each other or the boundary $\{r = 0\}$ during the time interval $[\bar{t}, \bar{t} + \Delta t]$. As the constant values of $A(t,r)$ do not change between such interactions, it follows that $\operatorname{Var} A(t)$ remains constant between interactions.

Finally, as $B(t,r)$ is piecewise affine in t it follows that $\operatorname{Var} B(t)$ increases at most at a linear rate between $\bar{t}$ and $\bar{t} + \Delta t$. Recalling that any discontinuity in the solutions under consideration separates states of the form $(a_-, b_- + ca_- t)$ and $(a_+, b_+ + ca_+ t)$, we obtain that

$$\operatorname{Var} B(\bar{t} + \Delta t) \leq \operatorname{Var} B(\bar{t}) + c\Delta t \cdot \operatorname{Var} A(\bar{t}).$$

4.1.4. Overall variation estimates. It follows from the analysis above that the solution $(A(t,r), B(t,r))$ of (2.13)-(2.14) with the piecewise constant initial data (4.1), satisfies the bounds (4.3)-(4.4) for all times $t_0 \geq 0$.

4.2. Initial data and their approximation. The variation bounds (4.3)-(4.4) provide a natural class of initial data (A_0, B_0) for which an argument based on scaling and Helly's theorem will yield existence of a corresponding weak solution. For this we define two "weighted" variations for any $A_0, B_0 \in L^\infty(\mathbb{R}_0^+)$ with $B_0(0) = 0$:

$$\mathcal{S}(A_0) = \sup \sum_{i=1}^{N} r_i |A_0(r_i) - A_0(r_{i-1})| \tag{4.5}$$

$$\mathcal{T}(B_0) = \sup \sum_{i=1}^{N} \tfrac{1}{r_i} |B_0(r_i) - B_0(r_{i-1})|, \tag{4.6}$$

where the supremums are taken over all finite, increasing selections in $\mathbb{R}^+$: $0 = r_0 < \cdots < r_N < \infty$. Also, define the (partial) energy integrals

$$\mathcal{E}(A_0) := \int_{\mathbb{R}^+} A_0^2(r)\, dr, \qquad \mathcal{F}(B_0) := \int_{\mathbb{R}^+} B_0^2(r)\, \tfrac{dr}{r^2}.$$

Then, according to (4.3)-(4.4), the relevant sets of initial data A_0 and B_0 for the AB-system (2.13)-(2.14) are

$$\mathcal{A} := \{A_0 : \mathbb{R}_0^+ \to \mathbb{R} \,|\, \operatorname{Var} A_0, \mathcal{S}(A_0), \mathcal{E}(A_0) < \infty\} \tag{4.7}$$

and

$$\mathcal{B} := \{B_0 : \mathbb{R}_0^+ \to \mathbb{R} \,|\, \operatorname{Var} B_0, \mathcal{T}(B_0), \mathcal{F}(B_0) < \infty\}, \tag{4.8}$$

respectively.

LEMMA 4.1. *Given $A \in \mathcal{A}$ and $B \in \mathcal{B}$. Then there are sequences (A_n) and (B_n) such that*

$$A_n \to A \text{ in } L^2(\mathbb{R}_0^+, dr), \quad B_n \to B \text{ in } L^2(\mathbb{R}_0^+, \tfrac{dr}{r^2}), \tag{4.9}$$

and such that for each integer $n > 0$:

(a) *$A_n(r)$ is piecewise constant, right-continuous, and $\operatorname{Var} A_n \le \operatorname{Var} A$, $\mathcal{S}(A_n) \le \mathcal{S}(A)$;*

(b) *$B_n(r)$ is piecewise constant, right-continuous, and $\operatorname{Var} B_n \le \operatorname{Var} B$, $\mathcal{T}(B_n) \le \mathcal{T}(B)$.*

Proof. Fix $A \in \mathcal{A}$ and $B \in \mathcal{B}$. We will show that there are sequences (A_n) and (B_n) satisfying (a) and (b) and such that

$$\|A - A_n\|_{L^2(\mathbb{R}_0^+, dr)} \le \tfrac{1}{n} \qquad \text{and} \qquad \|B - B_n\|_{L^2(\mathbb{R}_0^+, \frac{dr}{r^2})} \le \tfrac{1}{n}. \tag{4.10}$$

We follow [2] and start with A. First define the variation function

$$V(r) := \sup \Big\{ \sum_{j=1}^{N} |A(r_i) - A(r_{j-1})| \,\big|\, N \ge 1, 0 = r_0 < \cdots < r_N = r \Big\}. \tag{4.11}$$

By right continuity of $A(r)$, $V(r)$ is a right continuous, non-decreasing function satisfying

$$V(0) = 0, \qquad V(\infty) = \operatorname{Var} A. \tag{4.12}$$

For $\varepsilon > 0$, let $N = N(\varepsilon)$ be the largest integer $< \frac{\operatorname{Var} A}{\varepsilon}$ and set

$$r_0 := 0, \quad r_N := \infty, \quad r_j := \inf\{r : V(r) \ge j\varepsilon\}, \quad j = 1, \cdots, N-1. \tag{4.13}$$

Defining the function A^ε by

$$A^\varepsilon(r) := A(r_j) \quad \text{if } r \in [r_j, r_{j+1}), \quad j = 0, \ldots, N-1, \tag{4.14}$$

we obtain from (4.13) that

$$\|A^\varepsilon - A\|_{L^\infty(\mathbb{R}_0^+)} < \varepsilon. \tag{4.15}$$

By definition, A^ε is piecewise constant and takes values of the original function A. It follows that $\operatorname{Var} A^\varepsilon \leq \operatorname{Var} A$ and $\mathcal{S}(A^\varepsilon) \leq \mathcal{S}(A)$. Thus, for any $\varepsilon > 0$ the function A^ε satisfies (a) with the additional property (4.15).

We next use this to find an A_n satisfying (a) and also $(4.10)_1$. First, since $A \in L^2(\mathbb{R}_0^+, dr)$, for each n there is an η_n so that

$$\int_{\eta_n}^{\infty} A^2(r)\,dr < \tfrac{1}{2n^2}. \tag{4.16}$$

Now apply the argument above with $\varepsilon = \frac{1}{n\sqrt{2\eta_n}}$ to find a piecewise constant function $\tilde{A}_n$ satisfying (a) and with

$$\|A - \tilde{A}_n\|_{L^\infty(\mathbb{R}_0^+)} < \tfrac{1}{n\sqrt{2\eta_n}}. \tag{4.17}$$

We observe that, as $A \in L^2(\mathbb{R}_0^+, dr) \cap BV(\mathbb{R}_0^+)$, we have

$$\lim_{r\to\infty} A(r) = 0.$$

Now set

$$A_n(r) := \begin{cases} \tilde{A}_n(r) & r \in [0, \eta_n), \\ 0 & r \geq \eta_n. \end{cases} \tag{4.18}$$

A_n is piecewise constant and, by definition, takes values of $A(r)$. Thus (a) is satisfied, while $(4.10)_1$ follows from

$$\begin{aligned} \|A - A_n\|^2_{L^2(\mathbb{R}_0^+, dr)} &= \int_0^\infty |A(r) - A_n(r)|^2\,dr \\ &= \int_0^{\eta_n} |A(r) - \tilde{A}_n(r)|^2\,dr + \int_{\eta_n}^\infty A^2(r)\,dr \\ &\leq \int_0^{\eta_n} |A(r) - \tilde{A}_n(r)|^2\,dr + \tfrac{1}{2n^2} \qquad \text{(by (4.16))} \\ &\leq \eta_n \left(\tfrac{1}{n\sqrt{2\eta_n}}\right)^2 + \tfrac{1}{2n^2} = \tfrac{1}{n^2}. \qquad \text{(by (4.17))} \end{aligned}$$

A similar argument applies to B and yields $(4.10)_2$. ∎

4.3. Lipschitz continuity in time. We next show that the solutions constructed above define Lipschitz continuous maps from $\mathbb{R}_0^+$ into $L^1_{loc}(\mathbb{R}_0^+, dr)$. We fix $T > 0$ and piecewise constant data $A_0 \in \mathcal{A}$, $B_0 \in \mathcal{B}$ as in (4.1). Let $A(t,r)$, $B(t,r)$ denote the corresponding solutions. We shall first estimate

$$\|A(s') - A(s)\|_1 := \|A(s', r) - A(s, r)\|_{L^1(\mathbb{R}^+, dr)}$$

for times $0 \leq s < s' \leq T$, and we start with the situation when there are no interactions during the time interval $[s, s']$. The simplest case occurs when no front-location (i.e., position of a discontinuity) at time s is crossed by other fronts during $[s, s']$. The following lemma reduces the issue to this simplest case, for concreteness formulated for the A-component of the solution.

LEMMA 4.2. *With $A(t,r)$ as above, assume that no interaction occurs during the time interval $[s,s']$ where $0<s<s'\leq T$. Then, by letting M be a sufficiently large integer and setting*

$$\Delta t := \tfrac{s'-s}{M}, \tag{4.19}$$

we have: during each subinterval $(s+m\Delta t, s+(m+1)\Delta t]$, $m=0,\dots,M-1$, no front in $A(t,r)$ crosses any front location present at time $s+m\Delta t$.

Proof. Recall that $A(t,r)$ is piecewise constant for any t. For any $t\in[s,s']$, let $r_0(t):=0<r_1(t)<\cdots<r_N(t)$ denote the front locations in $A(t,r)$. As no interaction occurs during $[s,s']$ the minimal distance between adjacent fronts remains strictly positive, i.e.,

$$l := \min_{\substack{t\in[s,s'] \\ 1\leq i\leq N}} |r_i(t)-r_{i-1}(t)|>0.$$

Now let M be the smallest integer satisfying $M>\frac{c(s'-s)}{l}$. It follows that $c\Delta t<l$ and that any two adjacent fronts at time $t_m:=s+m\Delta t$ $(m=0,\dots,M-1)$ are at least a distance l apart. As each front is either stationary or moves a distance $c\Delta t<l$ during the time interval $I_m:=(t_m,t_{m+1}]$, it follows that during I_m no fronts cross a front location present at time t_m. ∎

Since discontinuities in $B(t,r)$ propagate with the same speeds $\pm c$, it is immediate that Lemma 4.2 applies with $A(t,r)$ replaced by $B(t,r)$.

LEMMA 4.3. *With the same setup as in Lemma 4.2 we have*

$$\|A(s')-A(s)\|_1 \leq c|s'-s|\cdot \operatorname{Var} A(s). \tag{4.20}$$

Proof. Define Δt as in (4.19). According to Lemma 4.2, and with the notation introduced in its proof, we have: as t increases from t_m to t_{m+1}, each front moves a distance $c\Delta t$ without crossing any front location present at time t_m. As the constant values taken by $A(t,r)$ do not change due to the absence of interactions during $[s,s']$, it follows that

$$\|A(t_{m+1})-A(t_m)\|_1 = c\Delta t\cdot \operatorname{Var} A(t_m).$$

Summing for $0\leq m\leq M-1$, and using that $\operatorname{Var} A(t)$ is constant, we obtain

$$\begin{aligned}\|A(s')-A(s)\|_1 &\leq \sum_{m=0}^{M-1}\|A(t_{m+1})-A(t_m)\|_1\\ &= \sum_{m=0}^{M-1} c|t_{m+1}-t_m|\cdot \operatorname{Var} A(t_m)\leq c|s'-s|\cdot \operatorname{Var} A(s).\end{aligned}$$

∎

The corresponding estimate for $B(t,r)$ requires a separate analysis since its values change with time. In particular, we need to restrict to a compact spatial domain. For $R>0$, we set

$$\|B(s')-B(s)\|_{1,R} := \|B(s',r)-B(s,r)\|_{L^1([0,R],dr)}.$$

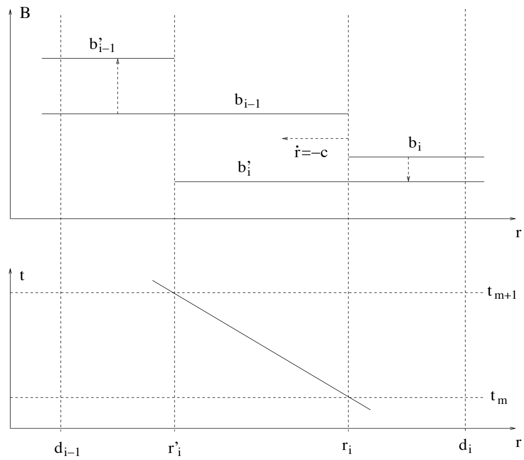

FIG. 4.1. *B-values (top) and front locations (bottom) in $J_i=(d_{i-1},d_i]$ during (t_m,t_{m+1}).*

LEMMA 4.4. *With $B(t,r)$ as above, assume that no interaction occurs during the time interval $[s,s']$ where $0<s<s'\le T$. Then, for any $R>0$ there is a number $L_{R,T}(A_0,B_0)$, depending only on R, T, and the initial data A_0 and B_0 (see (4.22)), such that*

$$\|B(s')-B(s)\|_{1,R}\le L_{R,T}(A_0,B_0)\cdot|s'-s|. \tag{4.21}$$

Proof. Recall that Lemma 4.2 applies to $B(t,r)$; using the notation introduced in its proof we first consider one of the subintervals $I_m=(t_m,t_{m+1}]$ $(m=0,\dots,M-1)$ in which no front crosses a front location present at time t_m. Without loss of generality we can assume that no fronts cross the location $r=R$ within the open interval (t_m,t_{m+1}). (If a front does meet $r=R$ at some time $\bar t\in(s,s')$, we add $\bar t$ to the t_m and rename them.)

Let $0<r_1<\cdots<r_N$ be the front locations in $[0,R]$ at time t_m. With $r_0:=0$ and $r_{N+1}:=R$, let

$$A(t_m,r)=\sum_{i=0}^N a_i\chi_{[r_i,r_{i+1})}(r),\qquad B(t_m,r)=\sum_{i=0}^N b_i\chi_{[r_i,r_{i+1})}(r),$$

for $0\le r\le R$. As no interactions occur between times t_m and t_{m+1} we have

$$A(t_{m+1},r)=\sum_{i=0}^N a_i\chi_{[r_i',r_{i+1}')}(r),\qquad B(t_{m+1},r)=\sum_{i=0}^N b_i'\chi_{[r_i',r_{i+1}')}(r),$$

where $r_i'=r_i+c_i\Delta t$ $(\Delta t=(t_{m+1}-t_m))$ for $i=1,\dots,N$, $c_i=\pm c$, and $r_0'=0$, $r_{N+1}'=R$. Also, $b_i'=b_i+a_ic\Delta t$ for $i=0,\dots,N$.

By our choice of the times t_m there is a partition $0=d_0<\cdots<d_N=R$ of $[0,R]$ such that $r_i,r_i'\in J_i:=(d_{i-1},d_i]$ for $i=1,\dots,N$. We first consider one of the intervals J_i, assuming for concreteness that $r_i'<r_i$. Referring to Figure 4.1, which depicts the situation where $a_{i-1}>0>a_i$, we have

$$\begin{aligned}
&\|B(t_{m+1})-B(t_m)\|_{L^1(J_i,dr)}\\
&=|b_{i-1}'-b_{i-1}|(r_i'-d_{i-1})+|b_{i-1}-b_i'|(r_i-r_i')+|b_i'-b_i|(d_i-r_i)\\
&=c\,[|a_{i-1}|(r_i'-d_{i-1})+|b_{i-1}-b_i'|+|a_i|(d_i-r_i)]\,\Delta t
\end{aligned}$$

$$
\begin{aligned}
&\le c\left[|a_{i-1}|(r_i'-d_{i-1})+|b_{i-1}-b_{i-1}'|+|b_{i-1}'-b_i'|+|a_i|(d_i-r_i)\right]\Delta t\\
&=c\left[|a_{i-1}|(r_i'-d_{i-1})+|a_{i-1}|c\Delta t+|b_{i-1}'-b_i'|+|a_i|(d_i-r_i)\right]\Delta t\\
&=c\left[|a_{i-1}|(r_i-d_{i-1})+|b_{i-1}'-b_i'|+|a_i|(d_i-r_i)\right]\Delta t\\
&=c\Big[\operatorname{Var}_{J_i}B(t_{m+1})+\int_{J_i}|A(t_m,r)|\,dr\Big]\Delta t,
\end{aligned}
$$

where Var_{J_i} denotes spatial variation over the interval J_i. Summing up the contributions from each J_i, we obtain

$$
\|B(t_{m+1})-B(t_m)\|_{1,R}\le c\Big[\operatorname{Var}_{[0,R]}B(t_{m+1})+\int_{[0,R]}|A(t_m,r)|\,dr\Big]\Delta t.
$$

Estimating the last integral in terms of the energy,

$$
\int_{[0,R]}|A(t_m,r)|\,dr\le R^{\frac{1}{2}}\Big[\int_{[0,R]}|A(t_m,r)|^2\,dr\Big]^{\frac{1}{2}}\le R^{\frac{1}{2}}\left[\mathcal{E}(A_0)+\mathcal{F}(B_0)\right]^{\frac{1}{2}},
$$

and using (4.4), show that $\|B(t_{m+1})-B(t_m)\|_{1,R}$ is bounded by

$$
c\Big[W(A_0,B_0)+cs'V(A_0,B_0)+R^{\frac{1}{2}}\left[\mathcal{E}(A_0)+\mathcal{F}(B_0)\right]^{\frac{1}{2}}\Big]\Delta t,
$$

where $V(A_0,B_0)$ and $W(A_0,B_0)$ were defined in (4.3)-(4.4). Finally, summing up over the time intervals I_m, and using that $s'\le T$, we obtain

$$
\|B(s')-B(s)\|_{1,R}\le\sum_{m=0}^{M-1}\|B(t_{m+1})-B(t_m)\|_{1,R}\le L_{R,T}(A_0,B_0)\cdot|s'-s|,
$$

where

$$
L_{R,T}(A_0,B_0):=c\Big[W(A_0,B_0)+cT\cdot V(A_0,B_0)+R^{\frac{1}{2}}\left[\mathcal{E}(A_0)+\mathcal{F}(B_0)\right]^{\frac{1}{2}}\Big]. \tag{4.22}
$$

□

Next, assume that an interaction occurs between times s and s' $(0<s<s'<T)$, and consider $\|A(s')-A(s)\|_1$. First, assume that there is a single time $\bar{s}\in(s,s')$ at which one or more interactions occur, one of which could be the reflection of a front at $(t,r)=(\bar{s},0)$. As fronts move at speed $\pm c$, it is readily verified that $\|A(\bar{s}\pm\Delta t)-A(\bar{s})\|_1$, where $0<\Delta t<\min(s'-\bar{s},\bar{s}-s)$, is of order Δt. Applying Lemma 4.3, and the fact that $\operatorname{Var}A(t)$ is constant for $t>0$ (cf. Sections 4.1.2 and 4.1.3), we obtain

$$
\begin{aligned}
\|A(s')-A(s)\|_1\le&\|A(s')-A(\bar{s}+\Delta t)\|_1+\|A(\bar{s}+\Delta t)-A(\bar{s})\|_1\\
&+\|A(\bar{s})-A(\bar{s}-\Delta t)\|_1+\|A(\bar{s}-\Delta t)-A(s)\|_1\\
\le&c\operatorname{Var}A(\bar{s}+\Delta t)\cdot(s'-(\bar{s}+\Delta t))+O(\Delta t)\\
&+c\operatorname{Var}A(s)\cdot(\bar{s}-\Delta t-s)\\
\le&c\operatorname{Var}A(s)(s'-s-2\Delta t)+O(\Delta t).
\end{aligned}\tag{4.23}
$$

Sending $\Delta t\downarrow 0$ we conclude that (4.20) holds whenever $0<s<s'$ are times for which there is a single intermediate time of interaction(s).

Let now s and s' be arbitrary times with $0<s<s'$. As there are at most finitely many interactions occurring during the time interval $[s,s']$, we can partition it into a finite number of subintervals of the type just considered. Applying (4.20) to each

subinterval and using the triangle inequality show that (4.20) holds for any two positive times s,s'.

Finally, assume that $0=s<s'=t_0$, where t_0 is chosen small enough that no interaction occurs during the time interval $(0,t_0)$. With the data (4.1) and with notation as in Section 4.1.1 we then have

$$\|A(t_0)-A(0)\|_1=|a_0|ct_0+\sum_{i=1}^{N}(|\hat a_i-a_{i-1}|+|\hat a_i-a_i|)ct_0$$
$$\leq c\Big(\operatorname{Var}A_0+|a_0|+\sum_{i=1}^{N}\tfrac{1}{r_i}|[[b]]_i|\Big)t_0=ct_0\cdot V(A_0,B_0). \tag{4.24}$$

Combining the results above we conclude: for piecewise constant data $A_0\in\mathcal{A}$, $B_0\in\mathcal{B}$ of the form (4.1), the first component $A(t,r)$ of the solution of the AB-system (2.13)-(2.14) satisfies the Lipschitz estimate

$$\|A(s')-A(s)\|_1\leq c|s'-s|\cdot V(A_0,B_0)\quad\text{for any } s,s'\geq 0, \tag{4.25}$$

where $V(A_0,B_0)$ is given by (4.3).

Next, consider the second component $B(t,r)$ of the solution. As above, let $0<s<s'<T$ and assume first that there is a single time $\bar s\in(s,s')$ at which one or more interactions occur. Again it is readily verified that $\|B(\bar s\pm\Delta t)-B(\bar s)\|_1$, where $0<\Delta t<\min(s'-\bar s,\bar s-s)$, is of order Δt. Fixing an $R>0$ and applying Lemma 4.4 we thus have

$$\begin{aligned}\|B(s')-B(s)\|_{1,R}&\leq\|B(s')-B(\bar s+\Delta t)\|_1+\|B(\bar s+\Delta t)-B(\bar s)\|_1\\&\quad+\|B(\bar s)-B(\bar s-\Delta t)\|_1+\|B(\bar s-\Delta t)-B(s)\|_1\\&\leq L_{R,T}(A_0,B_0)\cdot(s'-(\bar s+\Delta t))+O(\Delta t)\\&\quad+L_{R,T}(A_0,B_0)\cdot(\bar s-\Delta t-s)\\&\leq L_{R,T}(A_0,B_0)(s'-s-2\Delta t)+O(\Delta t).\end{aligned} \tag{4.26}$$

Sending $\Delta t\downarrow 0$ we conclude that (4.21) holds whenever $0<s<s'$ are times for which there is a single intermediate time of interaction(s).

If s and s' are arbitrary times with $0<s<s'<T$ we argue as for $A(t,r)$ above and obtain that the estimate (4.21), with the Lipschitz constant $L_{R,T}(A_0,B_0)$ in (4.22), holds for any two positive times s,s'.

Finally, assume that $0=s<s'=t_0$, where t_0 is as above. Consider the initial data (4.1) and use notation as in Section 4.1.1. Letting j be the largest index such that $r_j<R$ and choosing, if necessary, t_0 small enough that the forward wave from $(t,r)=(0,r_j)$ does not reach $r=R$ before time t_0, we have (assuming $R<r_{j+1}$)

$$\begin{aligned}&\|B(t_0)-B(0)\|_{1,R}\\&=(r_1-2ct_0)|a_0|ct_0+\sum_{i=1}^{j-1}\big[|\hat b_i-b_{i-1}|+|\hat b_i-b_i|+|a_i|(r_{i+1}-r_i-2ct_0)\big]ct_0\\&\qquad+\big[|\hat b_j-b_{j-1}|+|\hat b_j-b_j|+|a_j|(R-r_j-2ct_0)\big]ct_0\\&\leq c\Big[\sum_{i=1}^{j}(|[[b]]_i|+r_i|[[a]]_i|)+|a_0|r_1+\sum_{i=1}^{j-1}|a_i|(r_{i+1}-r_i)+(R-r_j)|a_j|\Big]t_0\\&=c\Big[W(A_0,B_0)+\int_0^R|A_0(r)|\,dr\Big]t_0\leq c\Big[W(A_0,B_0)+R^{\frac12}\mathcal{E}(A_0)^{\frac12}\Big]t_0.\end{aligned} \tag{4.27}$$

(The same result is obtained if $R=r_{j+1}$.) We conclude: for fixed $R,T>0$ and piecewise constant data $A_0\in\mathcal{A}$, $B_0\in\mathcal{B}$ of the form (4.1), the B-component of the AB-system (2.13)-(2.14) satisfies the Lipschitz estimate

$$\|B(s')-B(s)\|_{L^1([0,R],dr)}\le L\cdot|s'-s|\quad\text{for any } s,s'\in[0,T], \tag{4.28}$$

with a Lipschitz constant L depending on R, T, A_0 and B_0:

$$L=\max\Big(L_{R,T}(A_0,B_0),c\Big[W(A_0,B_0)+R^{\frac{1}{2}}\mathcal{E}(A_0)^{\frac{1}{2}}\Big]\Big), \tag{4.29}$$

where $L_{R,T}(A_0,B_0)$ is given by (4.21).

4.4. Existence of Weak Solutions to the 3-d radial wave system.

LEMMA 4.5. *For initial data A_0,B_0 with $A_0\in\mathcal{A}$ and $B_0\in\mathcal{B}$ (see (4.7)-(4.8)), there exists a weak solution of the initial-boundary value problem for the AB-system in the sense of Definition 2.3.*

Proof. Given the data A_0, B_0, we choose sequences $(A_{n,0})$, $(B_{n,0})$ as in Lemma 4.1, and let $A_n(t,r)$, $B_n(t,r)$ denote the resulting weak solutions. Note that Lemma 4.1 in particular implies that

$$A_{n,0}\to A_0 \text{ in } L^1_{loc}(\mathbb{R}^+_0,dr),\quad B_{n,0}\to B_0 \text{ in } L^1_{loc}(\mathbb{R}^+_0,dr). \tag{4.30}$$

Now fix $R>0$ and $T>0$. The results in Section 4.1 show that $A_n(t)$ and $B_n(t)$, for $t\in[0,T]$, satisfy the uniform variation estimates (4.3)-(4.4) (with t_0 replaced by T). As $A_n(t,r)$ vanishes for sufficiently large r while $B_n(t,r)$ vanishes along $\{r=0\}$, these variation bounds also yield uniform bounds on $|A_n(t,r)|$ and $|B_n(t,r)|$ (again for $t\in[0,T]$). Finally, the results in Section 4.3 show that A_n and B_n satisfy a uniform Lipschitz estimate of the form

$$\|A_n(s')-A_n(s)\|_{L^1([0,R],dr)}+\|B_n(s')-B_n(s)\|_{L^1([0,R],dr)}\le L\cdot|s'-s|,$$

where L depends on R, T, as well as on upper bounds for $\operatorname{Var}A_{n,0}$, $\operatorname{Var}B_{n,0}$, $\mathcal{S}(A_{n,0})$, $\mathcal{T}(B_{n,0})$, $\mathcal{E}(A_{n,0})$ and $\mathcal{F}(B_{n,0})$. (Note: as $A_{n,0}(r)$ vanishes for large r, the term $|A_{n,0}(r)|$ which appears in the Lipschitz constant L through $L_{R,T}(A_0,B_0)$ in (4.29), can be estimated in terms of $\operatorname{Var}A_{n,0}$.) By Lemma 4.1, L is therefore bounded independently of n in terms of R, T, $\operatorname{Var}A_0$, $\operatorname{Var}B_0$, $\mathcal{S}(A_0)$, $\mathcal{T}(B_0)$, $\mathcal{E}(A_0)$ and $\mathcal{F}(B_0)$.

A standard argument based on Helly's Selection Theorem (see Theorem 2.4 in [2]) implies that there are subsequences, denoted $(A_{n'})$, $(B_{n'})$, and limit functions A, B such that

$$A_{n'}\to A \quad\text{and}\quad B_{n'}\to B \quad\text{in } L^1_{loc}([0,T]\times\mathbb{R}^+_0), \tag{4.31}$$

and such that

$$A_{n',0}\equiv A_{n'}(0)\to A(0)\quad\text{and}\quad B_{n',0}\equiv B_{n'}(0)\to B(0)\quad\text{in } L^1_{loc}(\mathbb{R}^+_0). \tag{4.32}$$

The same argument also shows that the limits A, B satisfy the bounds

$$\|A(s')-A(s)\|_{L^1([0,R],dr)}+\|B(s')-B(s)\|_{L^1([0,R],dr)}\le L\cdot|s'-s| \tag{4.33}$$

for all $R>0$, $s,s'\in[0,T]$. By (4.30), (4.32) we obtain $A(0)=A_0$, $B(0)=B_0$ as elements in $L^1_{loc}(\mathbb{R}^+_0)$. Finally, the limit functions $A(t,r)$ and $B(t,r)$ can be chosen to be right-continuous with respect to r at each fixed time t; and these "good versions" satisfy the variation bounds (4.3)-(4.4) for any t_0.

It is now straightforward to use linearity of the AB-system, together with energy conservation, to show that the full sequences (A_n), (B_n) converge to the limits A, B, respectively, in $L^1_{loc}([0,T]\times\mathbb{R}_0^+)$. It follows from this that A and B can be extended to globally defined functions in $L^1_{loc}(\mathbb{R}_0^+\times\mathbb{R}_0^+)$.

Finally, fix any test functions $\varphi\in C_c^\infty(\mathbb{R}\times\mathbb{R}_0^+)$, $\psi\in C_0^\infty(\mathbb{R}\times\mathbb{R}_0^+)$, and numbers $R,T>0$ such that both $\varphi(t,r)$ and $\psi(t,r)$ vanish identically whenever $r\geq R$ or $t\geq T$. As (2.15) and (2.16) hold with A and B replaced by A_n and B_n, respectively, for each n it follows from (4.31) that (A,B) is a weak solution of the initial boundary value problem for the AB-system according to Definition 2.3. □

We finally translate Lemma 4.5 into an existence result for the linearized radial Euler system (2.3). Due to linearity it is immediate to verify that if (A,B) is a weak solution with initial data $A_0(r),B_0(r)$ of the AB-system according to Definition 2.3, then

$$v(t,r):=\tfrac{1}{r}A(t,r),\quad w(t,r):=\tfrac{1}{r^2}B(t,r)$$

is a weak solution of (2.3) with initial data $v_0(r):=\frac{1}{r}A_0(r),w_0(r):=\frac{1}{r^2}B_0(r)$ according to Definition 2.2. To formulate concisely the existence result for (2.3) we define data classes $\mathcal{V}$, $\mathcal{W}$ corresponding to the classes $\mathcal{A}$, $\mathcal{B}$. Introduce the following functionals for functions $v_0,w_0:\mathbb{R}_0^+\to\mathbb{R}$ with $w_0(0)=0$:

$$\mathbb{S}(v_0):=\sup\sum_{i=1}^N r_i|r_iv_0(r_i)-r_{i-1}v_0(r_{i-1})| \tag{4.34}$$

$$\mathbb{T}(w_0):=\sup\sum_{i=1}^N \tfrac{1}{r_i}|r_i^2w_0(r_i)-r_{i-1}^2w_0(r_{i-1})|, \tag{4.35}$$

where the supremums are taken over all finite, increasing selections of points in $\mathbb{R}^+$: $0=r_0<\cdots<r_N<\infty$. Next, define the (partial) energy integrals

$$\mathbb{E}(v_0):=\int_{\mathbb{R}^+}v_0^2(r)r^2dr,\qquad \mathbb{F}(w_0):=\int_{\mathbb{R}^+}w_0^2(r)r^2dr.$$

Finally, define the data sets

$$\mathcal{V}:=\{v_0:\mathbb{R}_0^+\to\mathbb{R}\,|\,\mathrm{Var}(rv_0(r)),\mathbb{S}(v_0),\mathbb{E}(v_0)<\infty\}, \tag{4.36}$$

$$\mathcal{W}:=\{w_0:\mathbb{R}_0^+\to\mathbb{R}\,|\,\mathrm{Var}(r^2w_0(r)),\mathbb{T}(w_0),\mathbb{F}(w_0)<\infty\}. \tag{4.37}$$

Lemma 4.5 now yields the following result.

THEOREM 4.1. *For initial data $v_0\in\mathcal{V}$ and $w_0\in\mathcal{W}$ there exists a weak solution $(v(t,r),w(t,r))$ of the initial-boundary value problem for the 3-d radial linearized Euler system (2.3) according to Definition 2.2. In turn*

$$\rho(t,\mathbf{x}):=\tfrac{1}{c}v(t,|\mathbf{x}|)\qquad \mathbf{u}(t,\mathbf{x}):=\tfrac{1}{\bar\rho}w(t,|\mathbf{x}|)\tfrac{\mathbf{x}}{|\mathbf{x}|}$$

provides a weak solution of the 3-d linearized Euler system (2.5).

Acknowledgment. This work was supported in part by NSF awards DMS-1311353 and DMS-1813283 (Jenssen).

REFERENCES

[1] P. Brenner, *The Cauchy problem for symmetric hyperbolic systems in L_p*, Math. Scand., 19:27–37, 1966. 1, 1.1

[2] A. Bressan, *Hyperbolic Systems of Conservation Laws*, Oxford University Press, 2000. 4, 4.2, 4.4

[3] G. Chen and M. Perepelitsa, *Vanishing viscosity solutions of the compressible Euler equations with spherical symmetry and large initial data*, Commun. Math. Phys., 338:771–800, 2015. 1

[4] G. Chen and M. Schrecker, *Vanishing viscosity approach to the compressible Euler equations for transonic nozzle and spherically symmetric flows*, Arch. Ration. Mech. Anal., 229:1239–1279, 2018. 1

[5] C. Dafermos, *Hyperbolic Conservation Laws in Continuum Physics*, Springer-Verlag, Berlin, 2016. 4

[6] C. De Lellis, *Blowup of the BV norm in the multidimensional Keyfitz and Kranzer system*, Duke Math. J., 127(2):313–339, 2005. 1, 1.1, 3.2

[7] L. Evans, *Partial Differential Equations*, Amer. Math. Soc., Providence, RI, 2010. 1

[8] J. Glimm, *Solutions in the large for nonlinear hyperbolic systems of equations*, Commun. Pure Appl. Math., 18:697–715, 1965. 1.1

[9] K. Guderley, *Starke kugelige und zylindrische Verdichtungsstgsse in der Niihe des Kugelmittelspunktes bzw. der Zylinderachse*, Luftfahrt-Forsch., 19:302–312, 1942. 1

[10] D. Hoff, *Spherically symmetric solutions of the Navier-Stokes equations for compressible, isothermal flow with large, discontinuous initial data*, Indiana Univ. Math. J., 14:1225-1302, 1992. 2.1

[11] H. Holden and N. Risebro, *Front Tracking for Hyperbolic Conservation Laws*, Springer, Heidelberg, 2015. 4

[12] G. Holzegeland, S. Klainerman, J. Speck, and W. Wong, *Small-data shock formation in solutions to 3D quasilinear wave equations: an overview*, J. Hyperbolic Differ. Equ., 13(1):1–105, 2016. 1

[13] X. Liu and P. Lax, *Positive schemes for solving multi-dimensional hyperbolic systems of conservation laws. II*, J. Comput. Phys., 187:428–440, 2003. 1

[14] R. Lazarus, *Self-similar solutions for converging shocks and collapsing cavities*, SIAM J. Numer. Anal., 18(2):316–371, 1981. 1

[15] P. LeFloch and M. Westdickenberg, *Finite energy solutions to the isentropic Euler equations with geometric effects*, J. Math. Pures Appl., 88(5):389–429, 2007. 1

[16] G. Leoni, *A First Course in Sobolev Spaces*, Amer. Math. Soc., Providence, RI, 2009. 1, 3.1

[17] W. Littman, *The non-existence of certain estimates for the wave equation*, in R.E. Langer (ed.), Partial Differential Equations and Continuum Mechanics, Univ. Wisconsin Press, Madison, 360–362, 1961. 1

[18] W. Littman, *The wave operator and L_p norms*, J. Math. Mech., 12:55–68, 1963. 1

[19] J. Rauch, *BV estimates fail for most quasilinear hyperbolic systems in dimensions greater than one*, Commun. Math. Phys., 106(3):481–484, 1986. 1, 1.1

[20] M. Schrecker, *Spherically symmetric solutions of the multidimensional, compressible, isentropic Euler equations*, Trans. Amer. Math. Soc., 373(1):727–746, 2020. 1